The Purification and Thermal Stability of the Peroxidase Enzyme in *Cucurbita moschata*

Garen Hamner

A Senior Thesis submitted in partial fulfillment
of the requirements for graduation
in the Honors Program
Liberty University
Spring 2024

Acceptance of Senior Honors Thesis

This Senior Honors Thesis is accepted in partial
fulfillment of the requirements for graduation from the
Honors Program of Liberty University.

_____
Gregory M. Raner, Ph.D.
Thesis Chair

_____
Michael Bender, Ph.D.
Committee Member

_____
James H. Nutter, D.A.
Honors Director

_____
Date

Abstract

Peroxidases are enzymes that catalyze the reduction of hydrogen peroxide to water while oxidizing organic substrates and are valuable in spheres like industrial and medical applications and histochemistry. Limitations still exist in the use of the well-studied horseradish peroxidase for certain activities due to limitations like poor thermal stability, thus the search for novel peroxidases that can overcome these limitations is an active area of research. Butternut squash peroxidase *(Cucurbita moschata)* (BSP) shows promise due to significant activity being found in the skin and apparent enhanced thermal stability, but an efficient purification scheme for it is lacking, as well as a detailed characterization of its thermal stability. The preliminary steps of a purification scheme for BSP were developed through methods like “salting out” precipitation techniques, affinity chromatography, and size exclusion chromatography. The efficacy of these techniques was evaluated through two assays. A kinetic assay served to quantify units of activity. A Bradford assay method used an external standard calibration curve to calculate the protein content of samples. The combination of these assays resulted in specific activity measurements that were used to assess the purity of the sample and show the effectiveness of the purification techniques. The thermal stability of BSP was then analyzed and compared to that of HRP, showing that BSP has a higher thermal stability than HRP by 10-20 °C.

Keywords: peroxidase, butternut squash, purification, thermal stability, biochemical analysis

The Purification and Thermal Stability of Peroxidase Enzyme in *Cucurbita moschata*

Background

The study of enzymes is necessary in general due to their role in catalyzing reactions with great degrees of efficiency. One class of enzymes that is of biotechnological significance is the peroxidase enzyme family. These enzymes are used to, "…catalyze various oxidative reactions using hydrogen peroxide and other substrates as electron donors" (Twala et al., 2020, 344).

When extracted, peroxidases serve a variety of worthwhile applications, including biobleaching of paper (Biswas et al., 2020), the production of bioenergy (Twala et al., 2020), the decolorization of dyes (Min et al., 2015), removal of phenolic contaminants from water for wastewater treatment (Gore, 2017), and the detection of other enzymes and antigens through immunoassays and chemiluminescence (Alegria-Schaffer et al., 2009; Sakharov, 2001; Thorpe & Kricka, 1986). For this reason, they have been the subject of much study, including the best sources of them. Peroxidase enzymes take many different forms that have specialized uses and effectiveness. They are divided into three superfamilies, but even those are diverse, with amino acid sequences found to be highly variable among the members of the plant peroxidase superfamily, with less than 20% identity in the most divergent cases (Hiraga et al., 2001). Specifically, sources of peroxidase have been studied for characteristics applicable to analytical chemistry such as the general activity of the source, versatility, ease of purification, and cost of purification/enrichment (Zia et al., 2011).

Currently, horseradish peroxidase (HRP) is used extensively for diagnostics and histochemistry (Krainer & Glieder, 2015), and serves as a standard labeling and indicator enzyme in enzyme immunoassays (Gallati & Pracht, 1985). Its wide use in such applications is

due to its stability, accessibility, relatively low cost, and high activity. It is, for example, significantly less expensive than alkaline phosphatase, another popular alternative used in applications like the formation of immunoglobulin conjugates (Beyzavi et al., 1987). With all of this being said, multiple factors still stand to be improved such as cost, activity, and specialization.

One example of the demand for better peroxidases is explained by Pontsho Patricia Twala, where she comments on the use of peroxidases in microbial spheres: “Discovery of more thermally stable novel peroxidases with better properties such as tolerance to organic solvents, salts, and heavy metals are of paramount importance and further research needs to be explored” (Twala et al., 2020). This is due to the value of peroxidases in the biodegradation of plastic waste. Unfortunately, while there is a recognition of the need for better peroxidase sources, there is a lack in the literature of emphasis on looking for them, and with that comes substantial opportunity for productive and marketable research. Another example is one in which a discovered peroxidase could merely be more effective for one aspect of HRP’s traditional uses. For instance, in a western blot analysis, a primary antibody specific to a protein can be used to detect a small amount of a protein. This is because a secondary antibody attached to HRP binds to the primary antibody and releases a measurable signal (Alegria-Schaffer et al., 2009). In this mechanism, a variety of substrates can be detected, but differ widely in detection limits. These methods are already being looked at to determine the most effective and sensitive conditions (Thorpe & Kricka, 1986), and a new secondary antibody attached to a novel peroxidase with higher catalytic activity could be useful in this regard.

Members of the HRP family of peroxidases contain heme. Heme is an organic ring-shaped prosthetic group that can hold an iron molecule and is common in plant peroxidases due

to its essential function in the enzyme. A heme can aid in transferring electrons in the oxidation of an organic compound (Briley, 2021). A visualization of this group is shown in Figure 1 (Nuss et al., 2021).

Figure 1

Heme group of HRP

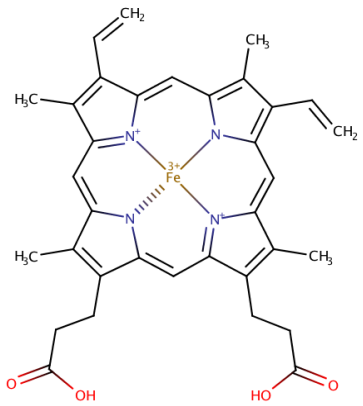

The presence of heme in peroxidases allows for a determination of peroxidase concentration. In a local study, Raner found a high activity of peroxidases in the skin of butternut squash as seen in Table 1 (Nuss et al., 2021). Upon further research, butternut squash was discovered to outperform HRP in a variety of tests. This gives it the potential to be used instead of HRP in traditional HRP functions.

Table 1

Heme concentration for purified samples

Sample	Concentration (μM)
Jalapeño Seeds (JAL-SD)	0.382
Zucchini Skin (ZUCS)	0.706
Butternut Squash (BTS)	0.859
Kabocha Squash (KOS)	0.913
Kudzu Leaf (KL)	0.529

This is where there is a shortcoming in the current understanding of BSP. While the methods of peroxidase purification have been well studied and refined for HRP (Spadiut & Herwig, 2013), the same cannot be said of butternut squash peroxidase (BSP). The methods used by Raner included a general purification process that could be used for all peroxidase sources. This process started with two ammonium sulfate precipitation steps, then a G50 Sephadex™ chromatography step, Amberlite™ resin purification, DEAE chromatography, and then another ammonium sulfate precipitation and G50 chromatography step. After the purification process had been employed, purity was checked by gel electrophoresis which indicates the separation of compounds by the existence of distinct electrophoretic bands. If there are multiple bands, it is clear that there are multiple proteins in the solution.

While Raner's team did manage to achieve a single electrophoretic band (Nuss et al., 2021), there were two problems. First, the band that was seen was not characterized as peroxidase, though it could be assumed that it was peroxidase due to the slight correlations between activity and the intensity of the band. The main problem is that the yield from the method was so low that it would be in no way practical to be employed to industrially produce pure BSP. This problem is illustrated by the lack of intensity of the electrophoretic line that was achieved, shown in Figure 2. It is evident from this research that a better purification scheme would need to be developed before BSP could be characterized and used industrially.

Figure 2

Demonstration of purification process through gel electrophoresis

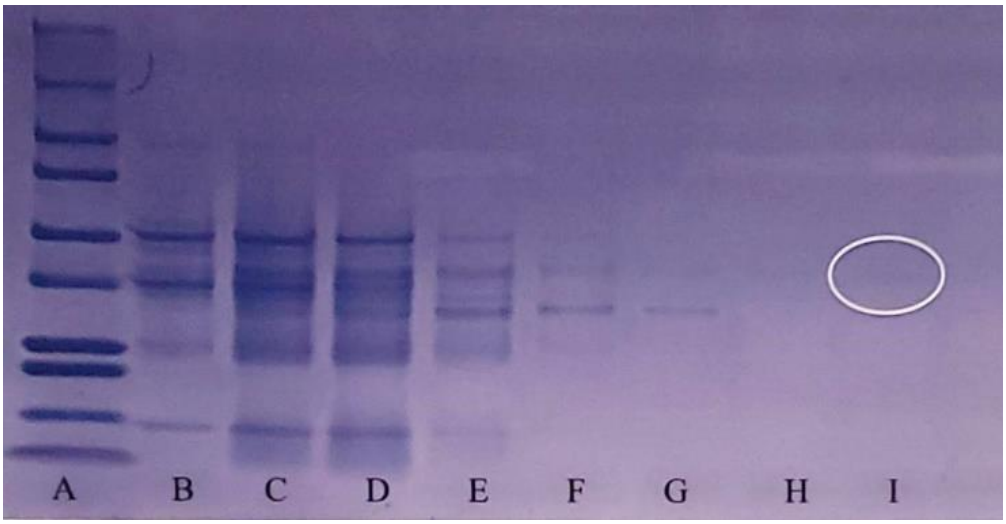

Thermal Stability

In the analysis of proteins, one common question is that of the limits of how and where it can be used. Some of those applications were explained above, but many of those relate to characterized properties of peroxidases. For instance, at some temperature, the forces that hold a protein in its secondary, tertiary, or quaternary structure are overcome and the protein becomes denatured. This is known as a protein's thermal stability. It is important to understand the thermal stability of proteins since some applications in biotechnology and food science, among others, require proteins to often be exposed to changes in temperature (Bischof & He, 2006; Leuenberger et al., 2017; Savitski et al., 2014).

Background knowledge about the thermal stability of peroxidases allows for comparison between experimental and literature thermal stability measurements and a framework from

which to interpret the relative thermal stability of BSP. Therefore, a literature review was conducted.

One fundamental article for the evaluation of thermal stability's role in the application of peroxidases is called "A Comprehensive Review on Function and Application of Plant Peroxidases" by Pandey (V. Pandey et al., 2017). The authors give a helpful overall diagram of the types of peroxidases mentioned earlier called superfamilies, shown in Figure 3.

Figure 3

Schematic representation of classification of peroxidases (V. Pandey et al., 2017).

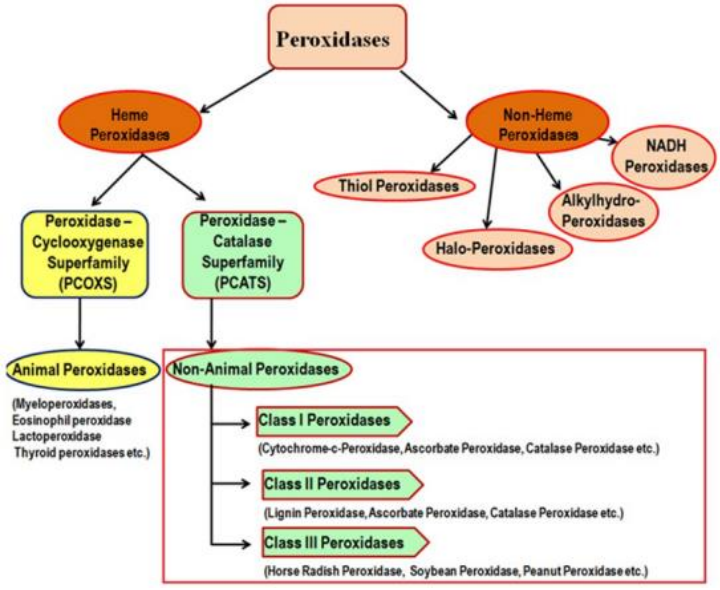

This schematic helps quickly narrow the scope of peroxidases to be analyzed. Plant peroxidases are found in Class III of the Peroxidase-Catalase Superfamily (PCATS). While there are some plant peroxidases found in the non-heme family like NADH peroxidase (Šimonovičová et al., 2004) and others in Class I (Passardi et al., 2004), the majority of the focus of the article is

found in Class III peroxidases. There are a plethora of ways in which peroxidases are used *in vivo* (Passardi et al., 2005), but thermal stability studies apply only to *in vitro* applications.

One prominent application of peroxidases is their use as biosensors. Biosensors are a special type of sensor that utilizes biochemical species to detect a certain signal, often in the form of a chemical (Bhalla et al., 2016). For instance, due to the peroxidase's functions and the reactions it catalyzes (Twala et al., 2020), it could be used very readily to detect the presence of hydrogen peroxide.

Specific research has been conducted in creating a hydrogen peroxide biosensor using soybean peroxidase (Vreeke et al., 1995). This biosensor was able to be operated at a temperature of 65 °C. This shows that there is a demand for the research already. The biosensor field is quite broad since there are any number of conditions in which analysis can be carried out. One example of a peroxidase sensor was fabricated with the use of nanoparticles and gel networks (Jia et al., 2002). This indicates additional peroxidase characteristics should be considered. For instance, HRP that has been adsorbed onto different materials like gold and sweet potato peroxidase shows a heightened electrochemical affinity (Jia et al., 2002; V. Pandey et al., 2017; Zhang et al., 2009). Alternatively, there are peroxidase sensors that have extended use in food applications like the detection of lactose in milk. These also need to be temperature stable (Sharma et al., 2002).

A category similar to that of biosensors is that of analytical and diagnostic kits. Both applications have intrinsic to them the detection of small amounts of a variety of analytes of interest. Pandey lists this as distinct from biosensors and claims that peroxidases which are both thermally stable and have a wide pH range could overtake HRP (V. Pandey et al., 2017). These kits are often seen in more biological applications (Malik & Pundir, 2002; Ragland et al., 2000).

While it might seem that this is an insignificant application, the sheer variety of analytes of interest that could be analyzed is staggering and leads to the conclusion that a thermal stability study is certainly needed.

Overview of Plant Peroxidases with Enhanced Thermal Stability

When overviewing the thermal stabilities of various peroxidases, the purpose of the literature review should be kept in mind. A review of thermal stabilities serves to give comparisons: (1) for how the peroxidase to be analyzed compares to current standards it is competing with, and (2) to grasp within what range a peroxidase should fall if it is to be considered as having satisfactory thermal stability. Since horseradish peroxidase (HRP) is the current standard for most applications, its stability should be analyzed. A fair representation is seen in Figure 4 below.

Figure 4

Profiles for the thermal stability of HRP and POL

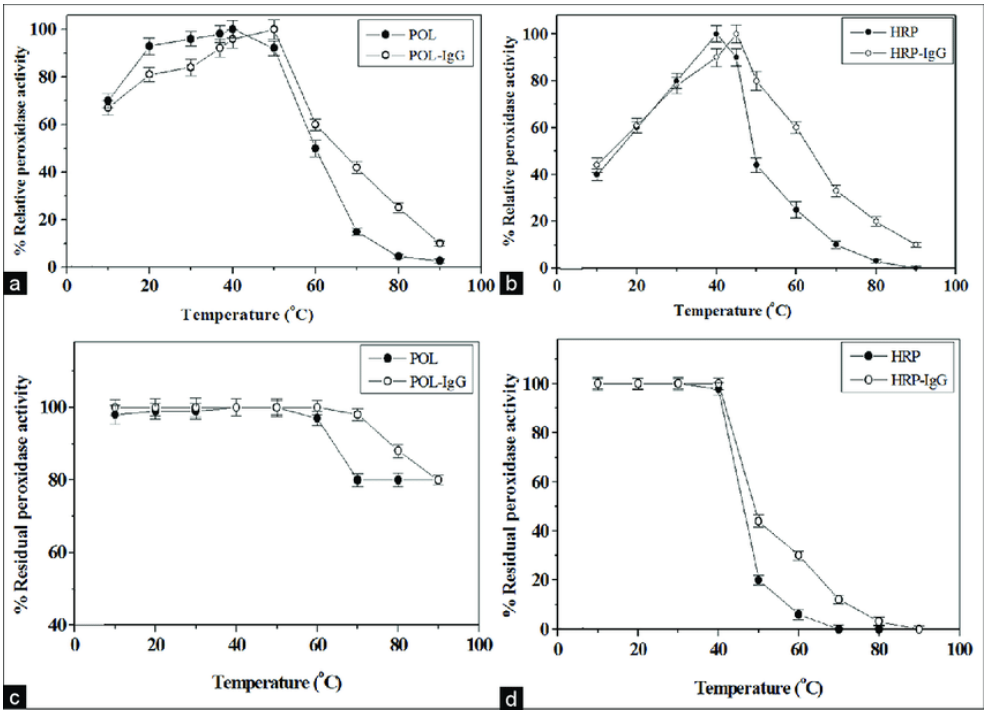

Note. Profiles for the assessment of the optimum temperature (a and b) and thermal stability (c and d) of the sycamore latex peroxidase (POL) and horseradish peroxidase (HRP) before and after the glutaraldehyde conjugation process. The values represent mean±standard error (n=4) (Abdel-Aty et al., 2018).

The subfigure of interest is Figure 2d. It clearly shows that HRP becomes denatured between 40 °C and 50 °C. This is a low stability, meaning that HRP is very limited in applications requiring temperature fluctuation like those mentioned above. In the current discussion, this assessment is based on the observation that there are peroxidases that remain active at much higher temperatures. Table 2 is a list of thermal stabilities observed for a series of selected plant peroxidases (V. Pandey et al., 2017).

Table 2

Thermal properties of some purified plant peroxidases

S. No.	Source	Temperature Optimum (°C)	Thermostability	References
1	*Carica papaya*	40	Retained 80% activity at 60 °C after 1 hr	(Singh et al., 2012)
2	*Roystonea regia*	-	Stable at 70 °C after 1 hr incubation	(Sakharov, 2001)
3	*Leucaena leucocephala*	55	Fully active at 65 °C for 20 min	(V. P. Pandey & Dwivedi, 2011)
4	*Eruca vesicaria sbsp. Sativa*	40	Retained 50% activity at 80 °C after 30 min incubation	(Nadaroglu et al., 2013)
5	*Citrus Medica*	50	Stable at 60 °C and 65 °C	(Mall et al., 2013)
6	*Brassica oleracea Var. Italica*	-	Stable at 80 °C after 1 hr incubation	(Thongsook & Barrett, 2005)

There are multiple plant peroxidases in this data that were shown to retain activity even at 80 °C, which was the highest temperature seen in a naturally occurring peroxidase. This

information sheds light on the fact that HRP is not highly stable at elevated temperatures. If a peroxidase could be found with stability at 60 °C or above, it could be said to have a significantly higher stability. More stable peroxidases are of such high desire that they have been designed using genetic engineering techniques (Barber-Zucker et al., 2022). The highest artificially made peroxidase ended up being stable up to 85 °C (Watanabe & Nakajima, 2016). Overall, it can be seen then that peroxidases find uses pertaining to higher temperature applications in enough ways to make a study of thermal stability significant.

Purpose of the Present Study

The purpose of this research was to develop a systematic approach for the purification of a peroxidase enzyme with observed higher thermal stability, namely the enzyme from butternut squash peroxidase. The first step of this purification involved ammonium sulfate precipitation, however refinement of this step was the first objective of the current study.

When conducting a purification, two key factors must be balanced: purity and recovery. In a purification scheme, a significant amount of purity could be attained, but if most of the sample is lost in the process of purification, the scheme is not reasonable. Similar processes of balancing these factors have been done in the refining of tomato peroxidase (Kokkinakis & Brooks, 1979), so it is reasonable to assume that it can be done for butternut squash. The method those authors used started with ammonium sulfate precipitation, then moved to ion exchange chromatography, and then two different assays. Polyacrylamide Gel Disc Electrophoresis and SDS-Polyacrylamide Gel Electrophoresis were used for characterization.

Once this purification is done, BSP can be more effectively characterized. For instance, k_{cat}, also known as the turnover number, “determines the reaction rate when the enzyme is fully occupied at a saturating concentration of the substrate” (Park, 2022, p. 2). In other words, k_{cat} is a

measure of the activity per molecule. The research becomes a lot more valuable if the peroxidase has a high k_{cat}, but that is identified once the sample has been purified. Currently, measurements for BSP activity in our prior research have not been precise, as seen earlier (Nuss et al., 2021).

While determining the k_{cat} would potentially show a general superiority of BSP over HRP, it is also possible that BSP could merely be more effective for one aspect of HRP's traditional uses, like that of western blot analysis (Alegria-Schaffer et al., 2009).

Effective purification schemes have already been developed for other peroxidase sources like tomato peroxidase (Kokkinakis & Brooks, 1979). The current study pursued three specific objectives. The first was to optimize the ammonium sulfate precipitation step. The second was to develop a purification scheme in which the effectiveness of both affinity chromatography (using phenyl Sepharose™) and size exclusion chromatography (using G50 Sephadex™) were employed. The third served the purpose of assessing the thermal stability of the enzyme by comparing it with HRP.

Methods

Initial Isolation and Centrifugation

Before the formal purification process began, it was necessary to initially isolate the part of the butternut squash that contained the peroxidase enzyme. It was known generally that peroxidases are found in the skin of many plants that exist close to the ground, specifically in the intermembrane space of the cell wall (Veljović Jovanović et al., 2018), so the sample was processed initially by removing the skin. A solution of 20 mM pH 7.0 potassium phosphate buffer was prepared to provide the appropriate matrix for the enzymes to be stable. The peel was blended in a blender with ~2.8 mL buffer/g skin and the product was decanted into 500 mL centrifuge bottles. The bottles were centrifuged in a Beckman Coulter Avanti J-25.50 centrifuge

at 8000 rpm for 30 minutes. The supernatant was decanted into a vessel, and then had its volume recorded, and was stored frozen until the next step.

Ammonium Sulfate Precipitation Gradient

Next, an ammonium sulfate precipitation was performed and refined. Ammonium sulfate precipitation employs a principle known as “salting out.” In this process, various concentrations of a salt are spiked into a solution with enzymes in it to disrupt the interactions with the solvent which keep the enzyme suspended in the solution. As a result, the enzymes interact more with each other (known as intermolecular interactions), becoming less soluble and precipitate out of the solution. Enzymes of smaller sizes will gradually precipitate as a higher percent saturation of ammonium sulfate (weight/volume) is attained.

In this case, the goal was to assess at what percent saturation there was the greatest increase in specific activity while minimizing activity loss, which is the fundamental principle of evaluating the purification process. The crude solution was separated into seven three mL fractions with the rest being saved. The solutions respectively had ammonium sulfate added to achieve 0-10, 0-20, 0-30, 0-40, 0-50, 0-60, and 0-70 percent saturation of ammonium sulfate, calculated using the data in Figure 5 and the volume of the fraction. The exact amount of ammonium sulfate added was weighed.

Figure 5

Ammonium sulfate precipitation chart

Initial concentration of ammonium sulfate (percentage saturation at 0 °C)	Percentage saturation at 0 °C																
	20	25	30	35	40	45	50	55	60	65	70	75	80	85	90	95	100
	Solid ammonium sulfate (g) to be added to 1 l of solution																
0	106	134	164	194	226	258	291	326	361	398	436	476	516	559	603	650	697
5	79	108	137	166	197	229	262	296	331	368	405	444	484	526	570	615	662
10	53	81	109	139	169	200	233	266	301	337	374	412	452	493	536	581	627
15	26	54	82	111	141	172	204	237	271	306	343	381	420	460	503	547	592
20	0	27	55	83	113	143	175	207	241	276	312	349	387	427	469	512	557
25		0	27	56	84	115	146	179	211	245	280	317	355	395	436	478	522
30			0	28	56	86	117	148	181	214	249	285	323	362	402	445	488
35				0	28	57	87	118	151	184	218	254	291	329	369	410	453
40					0	29	58	89	120	153	187	222	258	296	335	376	418
45						0	29	59	90	123	156	190	226	263	302	342	383
50							0	30	60	92	125	159	194	230	268	308	348
55								0	30	61	93	127	161	197	235	273	313
60									0	31	62	95	129	164	201	239	279
65										0	31	63	97	132	168	205	244
70											0	32	65	99	134	171	209
75												0	32	66	101	137	174
80													0	33	67	103	139
85														0	34	68	105
90															0	34	70
95																0	35
100																	0

[a] Reprinted from Englard and Seifter (1990), which was adapted from Dawson *et al.* (1969).

Note. The percent saturation seen as grams of solid ammonium sulfate to be added to one liter of solution was converted using the experimental volume of solution to calculate the experimental amount of ammonium sulfate to be added.

Each solution had the solid ammonium sulfate added slowly over the course of a few minutes while constantly being stirred on ice. Following a ten minute incubation on ice, each solution was then centrifuged in a Beckman Coulter Avanti J-25 centrifuge in a JA-25.50 case at 8000 rpm in microfuge tubes for 30 minutes at 4 °C. The supernatants were decanted and stored for specific activity analysis.

Specific Activity Evaluation

Quantitation of Specific Activity by Guaiacol Assay

The specific activity of every sample in the entire study was determined using the following two assays: a guaiacol (guai) assay and a Bradford (Brad) assay. Guaiacol is a

colorless reagent that acts as a substrate for peroxidase enzymes in a reaction with hydrogen peroxide. The product of this reaction is tetraguaiacol, which is a colored compound that is brownish orange with a maximum absorbance of 470 nm. This reaction is shown in Figure 6.

Figure 6

Reaction of guaiacol and H_2O_2 to create tetraguaiacol

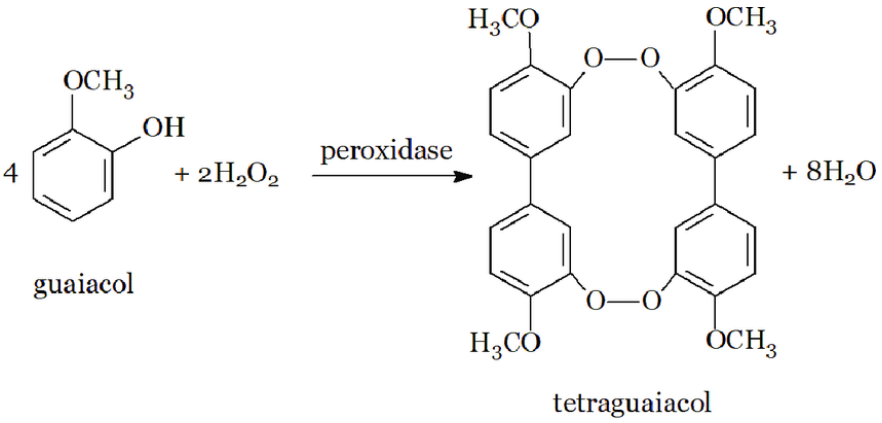

To assess the activity of a given peroxidase sample, one can add the sample to a solution of guaiacol, H_2O_2, and buffer and measure the kinetics (ΔAbs/min) via a UV-Vis Spectrometer. This can then be used along with the extinction coefficient of the tetraguaiacol (1 μmol / 0.0266 L) and the amount of sample in the reaction to obtain the activity per mL of reaction using equation 1.

$$\text{Activity (U/mL)} = (\Delta A/\text{min}) \times (1\ \mu\text{mol} / 0.0266\ \text{L}) \times (2) \times (0.001\ \text{L}) \times (1 / 0.01\ \text{mL}) \quad (1)$$

This U/mL can be used along with the initial volume of the solution to calculate the total activity of the solution. The activities of the samples were measured and recorded. For aliquots whose activities fell outside the linear range, dilutions were made and analyzed accordingly in the above manner.

Quantitation of Protein Content by Bradford Assay

The second assay performed, known as a Bradford assay, quantifies the total amount of protein in each sample. In this assay, the Bradford reagent reacts with the amide bond on any protein, turning a color with a maximum absorbance of 595 nm. In this assay 1000 μL of Bradford solution was added to cuvettes, followed by a 33 μL aliquot of each unknown sample. The cuvettes were then shaken vigorously and the reactions were allowed to proceed for five minutes. At the end of five minutes, solution absorbances were measured in an Thermo Fisher Scientific Genesys 10S UV-Vis spectrophotometer against a blank of 1.0 mL of Bradford reagent.

To convert absorbances to μg of protein / mL of solution, an external standard calibration curve was set up. A standard solution of 2000 μg/mL bovine serum albumin (BSA) was diluted to prepare a curve with protein concentrations ranging from 50 μg/mL up to 1000 μg/mL. The absorbances obtained from the assay were plotted and a linear regression was performed to calculate the equation of the line of best fit, which was used to calculate the protein content of the experimental samples. The protein concentration per mL measurement could be converted to μg of protein in all of a given sample in a similar fashion as the activity by multiplying by the initial volume of the sample. The percent activities from each percent saturation of ammonium sulfate were plotted and used to evaluate at what percent saturation the most effective recovery was obtained.

Full Purification

Another sample was then purified using the same initial isolation and centrifugation steps. The crude solution was not collected. A 0-40% ammonium sulfate saturation precipitation was performed since it was deemed to be the most efficient percent saturation for optimal protein

recovery. It was performed in the same manner mentioned above and processed in a Beckman Coulter Avanti J-25 centrifuge with a JLA-10.500 rotor at 8000 rpm for 30 min at 4 °C. A second centrifugation was used with this sample to ensure that precipitated proteins were taken out in the pellets. An aliquot of the supernatant from this sample was set aside for specific activity analysis. Samples were refrigerated when not being purified throughout the rest of the purification process.

Affinity Chromatography

Immediately after the second centrifugation, affinity chromatography was performed. An approximately 18-inch chromatography column was obtained. Around 1-2 inches of phenyl Sepharose™ was added to the column suspended in 20% ethanol. Once packed, 40% ammonium sulfate in deionized (DI) water was used to flush the column. After this solution reached the top of the gel, the sample was inserted and allowed to completely run into the gel and adsorb to it, having more 40% solution added on top of it. After it was fully loaded, fractions of decreasing saturations of ammonium sulfate were added to gradually elute off proteins with the specifications shown in Table 3.

Table 3

Volumes and percent saturations of affinity chromatography aliquots

Percent saturation	mL added
40	10
35	10
30	20
25	20
20	20
10	20
0	50

Aliquots were collected initially every ten mL, transitioning to every five mL once it was apparent by the color of the peroxidase that it was starting to elute off. After it had eluted the column was flushed with DI water. The fractions that contained larger amounts of peroxidase in them, based on color, had their specific activities analyzed.

Sample Concentration

The four highest specific activity fractions (collected when the following solutions had been added: 9 mL 10%, 14 mL 10%, 19 mL 10%, and start of DI) were combined and concentrated via a short phenyl Sepharose™ column. In this column, the four fractions were taken to 40% $(NH_4)_2SO_4$ so that they would adsorb to the column. Then they were flushed with DI water so that they would elute immediately. They were collected in one mL fractions.

Size Exclusion Chromatography

Size exclusion chromatography was then performed on the sample. A G50 Sephadex™ chromatography column that was around 11 cm long was created in a 20 mM pH 7.0 phosphate buffer. Once the column was packed and the buffer reached the top of the gel, the sample was added, and more buffer was added on top. Aliquots of one mL were collected once the peroxidase was nearing the bottom of the column. The fractions were then selectively analyzed for activity first and then narrowed further and tested for specific activity. These values were then plotted to visualize where the highest increase in specific activity was obtained.

At the end of the purification process, the activities and specific activities at each step were compared to calculate the total purification factor of the experiment and the percent recovery, and final procedural evaluations were performed as to the effectiveness of each purification step and future improvements to the procedure.

Thermal Stability

The 500 μL of each of the three highest activity fractions (12, 13, and 14) from the full purification were combined. The proper dilution factor for a guaiacol assay was determined, and samples at that dilution were prepared in duplicate and placed in a temperature controlled thermal plate. For each trial, duplicate samples had their activities measured via guaiacol assay every ten minutes for an hour. Reactions were started by removing an aliquot of enzyme from the thermal plate and adding it to prepared reaction mixture at room temperature assay conditions reported previously. Two trials each were done with BSP samples at 60 °C and 70 °C. Plots of activity vs. time were created to assess the thermal stability of the sample BSP. Three trials of HRP were done at 50 °C, and two trials were done at 60 °C. Results were plotted and compared to that of the BSP trials to assess the relative thermal stability of each peroxidase.

Results

Analytical Scale Purification Used for Method Development: Ammonium Sulfate Precipitation

Once the initial isolation and centrifugation were done, ~25 mL of crude solution was collected. The solution had a pale translucent yellowish-orange color. Other experiments within the Raner research team revealed that freezing the solution made the peroxidase have a lower activity than simply refrigerating the sample. Therefore, freezing samples was avoided in all subsequent steps. The solution was divided into seven three mL fractions with the rest saved as a crude sample.

The initial objective was to determine what percentage of AS would result in the highest recovery of peroxidase in the initial step. The amount of ammonium sulfate to be added according to Figure 3 and the actual amount added to each aliquot of sample is recorded in Table

3. For instance, for the 0-20 percent saturation solution, the table value of 106 g AS/L was multiplied by the volume of the solution to obtain 106 g AS/L * 0.003 L = 0.318 g AS to be added.

Table 3

Mass of ammonium sulfate (AS) added

Percent saturation	g AS/L	Exact g AS to add	Experimental g AS added
0-10	50	0.15	0.149
0-20	106	0.318	0.319
0-30	164	0.492	0.496
0-40	226	0.678	0.676
0-50	291	0.873	0.87
0-60	361	1.083	1.079
0-70	436	1.308	1.305

Guaiacol and Bradford assays were performed on each sample. Table 4 shows the results of the guaiacol assay with the ΔAbs/min converted to activity (U) per mL via Equation 1, which was then used to calculate the percent activity when compared with the highest activity measured (10% saturation). For example, for the 20% saturation sample, Activity (U/mL) = (0.864ΔA/min) * (1 μmol / 0.0266 L) * (2) * (0.001 L) * (1 / 0.01 mL) = 6.50 U/mL. When multiplied by three mL of solution, the total U of 19.49 was obtained. The percent activity was (19.49 U / 21.47 U) * 100% = 90.76%. The percent activities were plotted against the percent saturation in Figure 7. Based on the data in Figure 7, 40% saturation retained ~90% of the total peroxidase, while anything higher reduced this below 80%. Therefore the 40% saturation was selected as the first step in purification to retain over 90% of the original protein.

Table 4

Guaiacol assay experimental AS gradient results

Percent saturation	ΔAbs/min	Initial dilution (mL)	Extra dilution	U/mL	Total U	Percent activity
Crude	0.842	3	1	6.33	19.00	N/A
10	0.952	3	1	7.16	21.5	100
20	0.864	3	1	6.50	19.5	90.8
30	0.946	3	1	7.11	21.3	99.4
40	0.85	3	1	6.39	19.2	89.3
50	0.735	3	1	5.53	16.6	77.2
60	0.736	3	1	5.53	16.6	77.3
70	0.522	3	1	3.92	11.8	54.8

Note. No extra dilutions were used throughout the entirety of this experiment due to the rates of reaction always being linear.

Figure 7

Activity vs. percent saturation of AS gradient

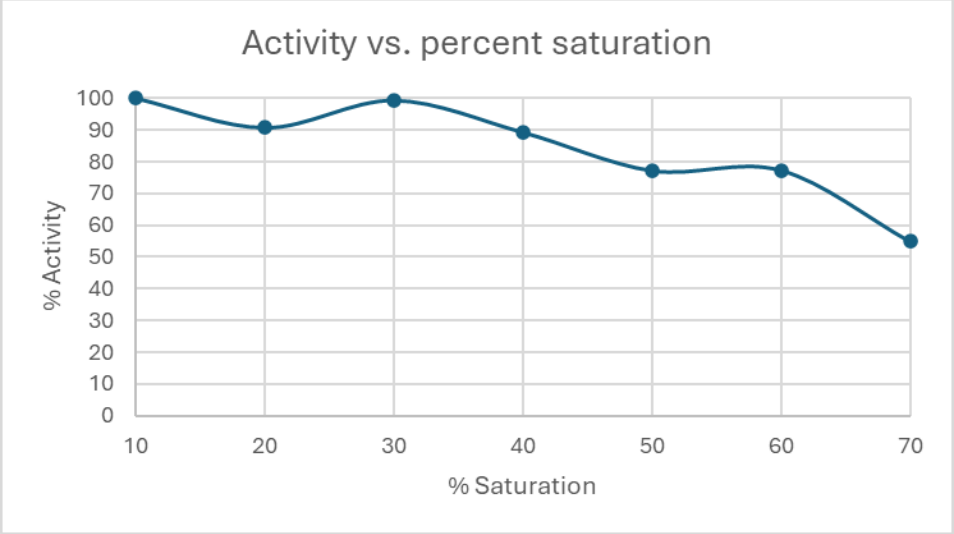

For the Bradford assay, a standard curve was prepared which was then used to calculate the protein concentrations in each sample. Table 5 lists the µg/mL of STDs along with their absorbances, which are plotted in Figure 8.

Table 5

Bradford assay calibration curve for AS gradient

Trial	µL BSA added	µL Brad added	µg/mL BSA	Absorbance at 595 nm
method blank	**0**	1000	0.00	0
1	**33.5**	1000	50.00	0.022
2	**33.5**	1000	100.00	0.068
3	**33.5**	1000	200.00	0.095
4	**33.5**	1000	400.00	0.171
5	**33.5**	1000	600.00	0.287
6	**33.5**	1000	800.00	0.377
7	**33.5**	1000	1000.00	0.533

Note. In the STD preparation, 33.5 µL of BSA STD was used for each reaction instead of the ideal 33.3 µL due to micropipette gradations not having more specific measurements. This difference was not accounted for in calculations due to being negligible.

Figure 8

BSA STD curve for AS gradient

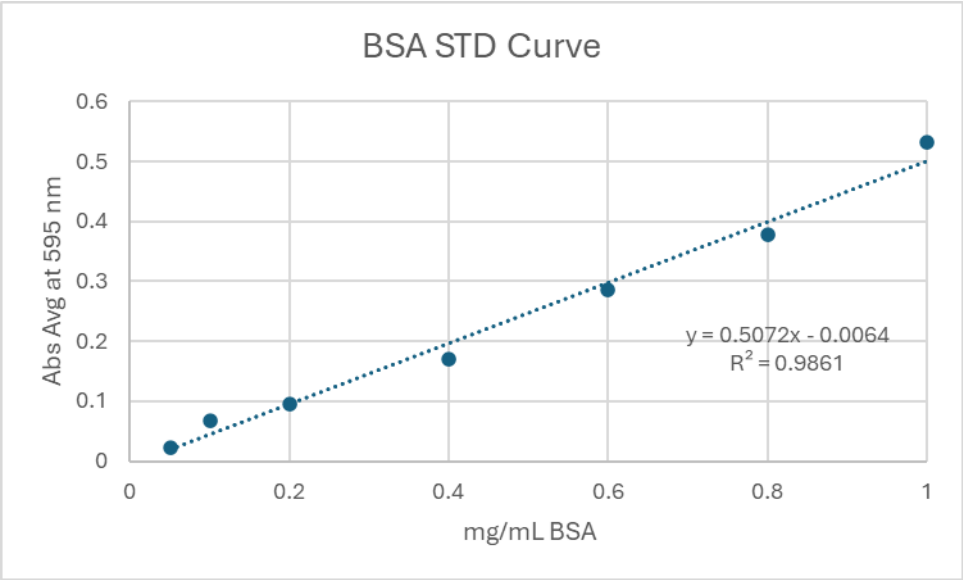

The µg/mL concentrations were converted to mg/mL concentrations for the m and b used to calculate the amount of protein in the samples. In the curve, slight non-linearity appeared toward the top of the curve, so samples with absorbances toward the top were viewed as not as accurate.

Table 6 shows the experimental Bradford assay results for the AS gradient, with the absorbance observed and the equivalent (eqv) µg/mL of protein. Sample protein concentrations were calculated by using m = 5.07×10^{-3} and b = -0.0064 from the standard curve in Figure 5, so µg/mL protein = $((\text{Abs} + 0.0064)/5.07 \times 10^{-3}) * (1000\ \mu g/mg)$.

Table 6

Bradford assay experimental AS gradient results

Percent saturation	mL sample added	mLBrad added	µg/mL eqv protein	Absorbance at 595 nm
Crude	**33.5**	1000	-15.0	-0.014
10	**33.5**	1000	0.789	-0.006
20	**33.5**	1000	36.3	0.012
30	**33.5**	1000	26.4	0.007
40	**33.5**	1000	30.4	0.009
50	**33.5**	1000	50.1	0.019
60	**33.5**	1000	73.7	0.031
70	**33.5**	1000	103	0.046

Note. The blank used was simply 1000 µL of Bradford solution without 33 µL of DI water added, which is the suspected reason for the negative absorption values throughout the calculations in the rest of the research.

The low absorbances for most solutions were below the absorbance threshold for the detection of protein of 0.030, which simply means that the amount of protein for each sample was less than ~ 70 µg/mL. Therefore, in the evaluation of the AS gradient, the loss of activity was the determining factor in deciding that the 0-40% saturation AS was the most appropriate experimental value to be used since it had a percent activity of about 90% and started to drop off more significantly after that point. Specific activity was not evaluated in this part of the experiment.

Large Scale Purification

The initial processing and centrifugation of the butternut skin sample yielded about 254 mL of crude solution. For the 0-40% AS precipitation it was determined that 57.404 g should be

added to the solution, and 57.407 g of AS was actually added. The 40% supernatant weighed 300.325 g.

Affinity Chromatography

The 40% AS sample was loaded onto a preparative phenyl Sepharose™ column prepared with 40% AS. For the affinity chromatography, it was observed that elution started happening slowly at 30% saturation AS, and more quickly at 25%. Therefore 25-30% saturation was chosen as the preferred range for peroxidase elution. The volumes of the fractions collected, the solutions that were being added to the top of the column when they were collected, and the summarized results of the subsequent guaiacol and Bradford assays which were used to calculate the specific activity are all shown in Table 7. The specific activity was calculated by dividing the U/mL by the mg/mL of protein to obtain the U/mg of protein. For instance, when the fourth mL of the 10% saturation AS solution was being added to the top of the column, the specific activity was 151.95 U/mL / [434.72 μg/mL protein * (1 mg / 1000 μg protein)] = 349.55 U/mg. The increase in factor of specific activity was then calculated by dividing each specific activity by the specific activity of the crude solution. For the same example, the increase in specific activity was 349.55 U/mg / 124.93 U/mg = 2.80.

Table 7

Affinity chromatography results

Fraction	mL of sample	U/mL	Total U	µg/ml protein	mg protein	U/mg protein	Increase in U/mg
Crude	300	41.8	12537	335	100	125	N/A
14.5mL 20%	5	21.8	109	N/A	N/A	N/A	N/A
19.5mL 20%	5	44.3	222	N/A	N/A	N/A	N/A
10% at 4mL	5	152	760	435	2.17	350	2.80
9mL 10%	5	323	1617	744	3.72	435	3.48
14mL 10%	5	304	1521	707	3.54	430	3.44
19mL 10%	5	300	1501	559	2.79	537	4.30
start of DI	5	470	2350	776	3.88	605	4.85
~10mL	10.4	178	1852	690	7.18	258	2.07

Note. The guaiacol assays were performed first, and only the fractions with substantial increases in U/mL had Bradford assays performed.

It was determined through Table 7 results that the 9 mL 10%, 14 mL 10%, 19 mL 10%, and start of DI fractions were the purest, and thus these fractions were combined and concentrated. The average specific activity of these fractions, and therefore the assumed specific activity of the concentrated solution, was 501.86 U/mg protein, being an increase in specific activity by a factor of 4.02. The total yield at this point was 55.75% based on the total in the crude sample.

Size Exclusion Chromatography

In the size exclusion chromatography (SEC), 26 total one mL fractions were acquired. The activities of a broad sampling of fractions are shown in Figure 9.

Figure 9

Activities of a broad sampling of SEC fractions

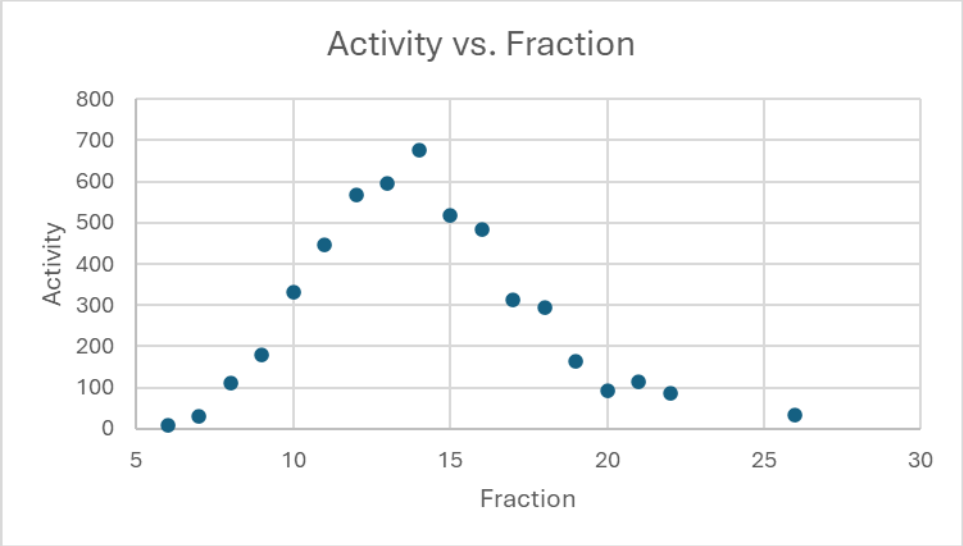

From this plot, samples at either end of the peak had their protein content assessed, shown in Figure 10.

Figure 10

Protein content of a sampling of SEC fractions

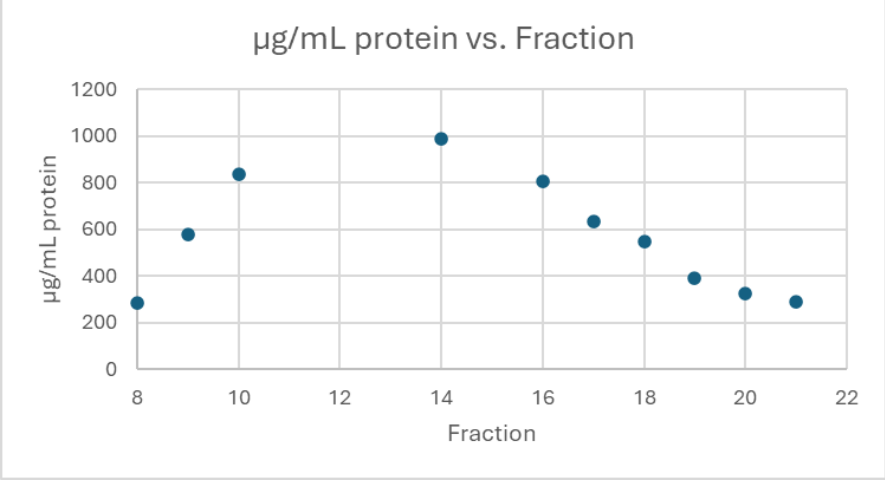

When compared with the µg/mL of protein seen in Figure 7, the protein content of the SEC fractions was not significantly lower than the affinity chromatography fractions, indicating a lack of purification with this step. The combination of the activity and protein content to obtain the specific activity is found in Table 8. Figure 11 shows the relationship between the fraction and specific activity in graphical format.

Table 8

Size exclusion chromatography results

Fraction	U/mL	µg/ml protein	U/mg protein
8	111	284	392
9	178	581	306
10	331	839	395
14	677	989	684
16	484	805	601
17	314	636	493
18	296	546	542
19	165	394	418
20	92	324	286
21	115	292	394

Figure 11

Specific activity vs. fraction SEC results

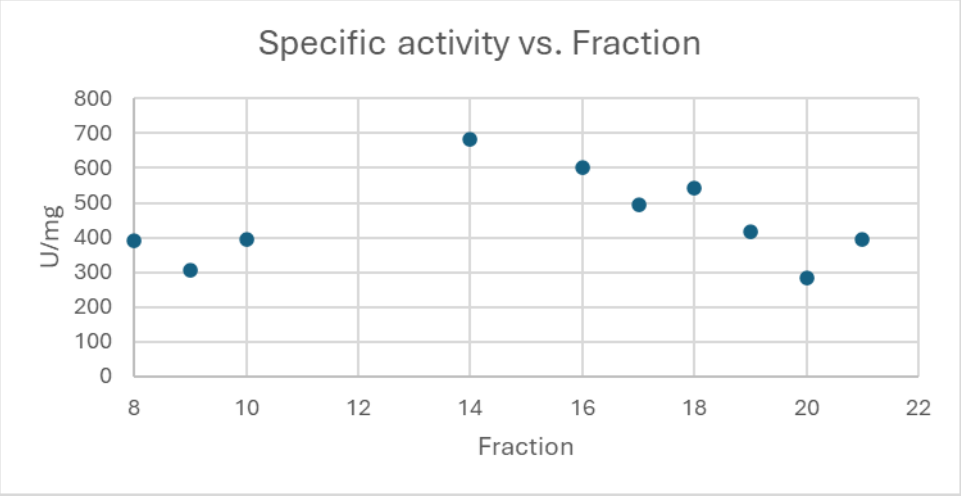

Table 8 shows that significant gains in specific activity were not achieved with the size exclusion chromatography with a G50 Sephadex resin. The maximum specific activity seen was 684 U/mg protein. While the fractions immediately surrounding this fraction could have had high specific activities, this is unlikely when the plots of the activity and protein content are compared. The curves are similar enough to assume that the full specific activity plot would be similar in form to the activity plot.

Purification Summary

At the end of the purification, the fractions from each purification step that were most effective were evaluated for their increase in specific activity and relative recovery, shown in Table 9. The increase in specific activity was calculated by dividing the final specific activity for each fraction by the specific activity of the 40% supernatant from the AS precipitation due to a crude aliquot not being obtained. For instance, for the affinity chromatography combination, the increase in U/mg = 501.67/124.93 = 4.02. The percent recovery of each step was calculated using a comparison with the estimated total activity of the crude sample.

Table 9

Final purification effectiveness measurements

Method	Fraction	Total U	mg protein	U/mg protein	Increase in U/mg	Recovery (%)
AS Precipitation	Crude	14000	N/A	N/A	N/A	N/A
	40% supernatant	12500	100	125	**N/A**	**89.3**
Affinity Chromatography	9mL 10%	1617	3.72	435	3.48	12.9
	14mL 10%	1521	3.54	430	3.44	12.1
	19mL 10%	1501	2.79	537	4.30	12.0
	start of DI water	2350	3.88	605	4.85	18.7
	Combination	6989	13.9	502	**4.02**	**55.8**
G50 Size Exclusion	14	677	0.99	684	5.48	9.69
	16	484	0.81	601	4.81	6.92
	17	314	0.64	493	3.95	4.49
	18	296	0.55	542	4.34	4.23
	Combination	1770	2.98	595	**4.76**	**25.3**

Note. The crude activity was estimated by taking the percent recovery from the AS gradient at 40% saturation of 89.3% and assuming that was the same percent recovery for the full purification. The data for the combination fractions were obtained by taking the sum of the activity, protein content, and recovery and averaging the increase in U/mg.

It should be noted that since the goal of the G50 Sephadex size exclusion chromatography was not to assess the exact increase in U/mg but rather to determine the range of fractions that would be combined in future steps, the data set is incomplete. Fractions 11-13 and 15 are not present. While the specific activity of fraction 10 was not higher than the specific activity going into that step, fractions 11-13 would likely have had specific activities that would deem them usable as can be inferred by the trend of the specific activities seen. The percent recovery in the size exclusion chromatography step if fractions 11-13 and 15 were included would be 27.8%.

Thermal Stability

Figure 12 displays the results of the BSP thermal stability trials with trendlines fitted to each trial. The thermal stability test of BSP revealed that it shows complete stability at 60 °C, with a significant loss of activity at 70 °C.

Figure 12

BSP thermal stability plot

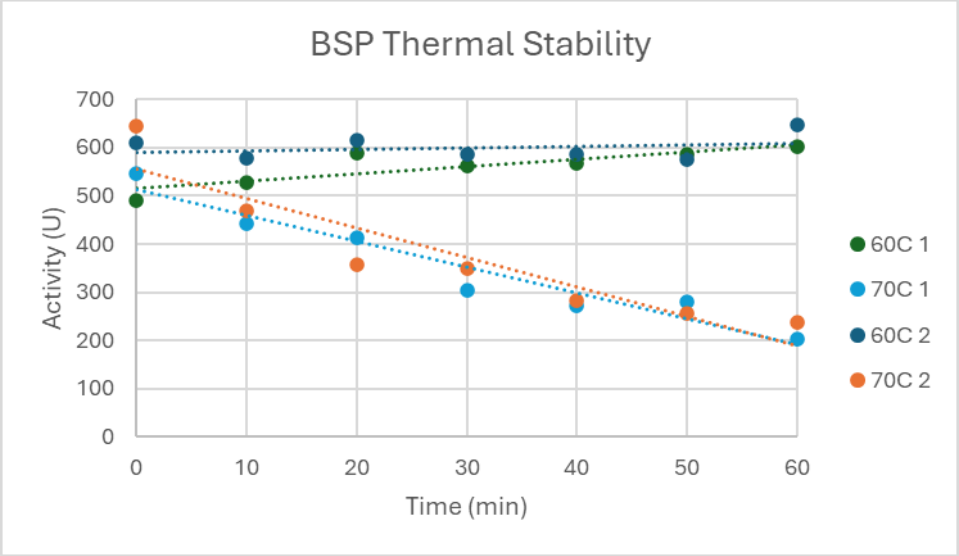

Figure 13 displays the results of the HRP thermal stability trials with trendlines fitted to each trial. The thermal stability test of HRP revealed that it shows stability at 50 °C, with a significant loss of activity at 60 °C. Figure 14 is a plot of the averages of the residual activities seen in Figures 12 and 13 for each trial.

Figure 13

HRP thermal stability plot

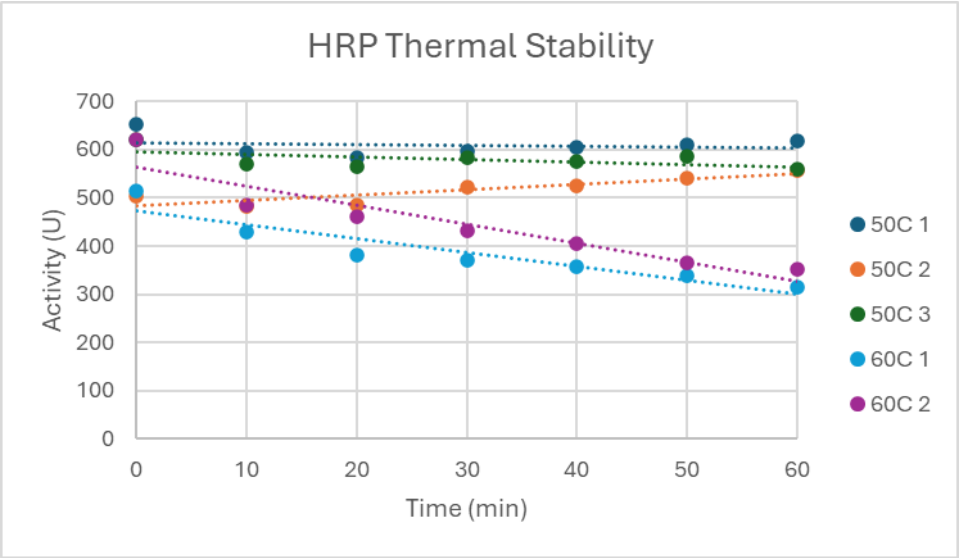

Figure 14

Profiles for the thermal stability of HRP and BSP

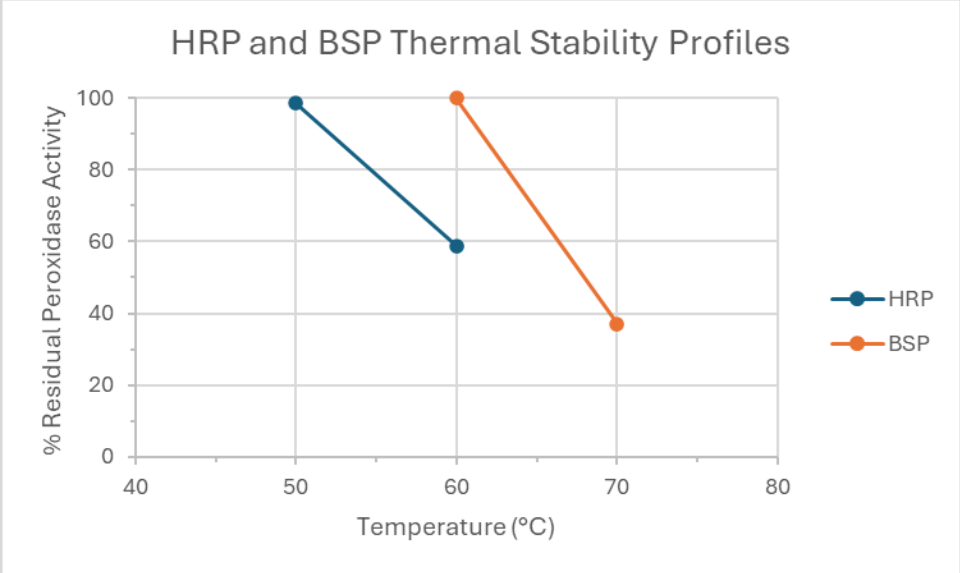

The insights gleaned from Figures 12 and 13 are solidified through what is seen in Figure 14. Due to the first two 50 °C HRP trials conflicting significantly in percent loss, a third trial that was done led to the belief that there is little to no loss of activity at 50 °C. This would at most indicate that the precise thermal stability of HRP is closer to 50 °C than 60 °C. There was technically a significant percent gain of activity in the 60 °C BSP Trials which indicates experimental error, but despite that it is evident that there was no significant loss of activity at 60 °C. Based on this data, it therefore seems safe to conclude that BSP has at least a 10 °C higher thermal stability than HRP.

Discussion

From the ammonium sulfate precipitation gradient experiment, it was determined confidently that the 0-40% saturation step was the best first purification step. An extra experiment would need to be done to show the factor of purification that is involved in the process. In the most extensive purification, it was discovered that refrigerating peroxidase samples led to a greater preservation of activity than freezing.

Overall, affinity chromatography was demonstrated to be an effective step since it yielded a five-fold purification with an approximately 55% recovery. If the chromatography were to be done more gradually, a higher recovery could potentially be achieved. For instance, since the elution started happening at 30% saturation with a quicker elution at 25%, affinity chromatography could be done that employed a more significant amount of solution at 35% saturation like 50 mL. Then, since it was seen that most of the BSP had eluted by the time the DI water was added, which was 80 mL of gradually diluted AS solution later, 100-150 mL of 25% saturated solution could be added to fully elute the BSP with fewer contaminating enzymes. The chromatography column would be cleaned with copious amounts of DI water afterward. While

the eluted fractions of BSP would be very dilute, they could easily be concentrated as was done in this experiment by a short phenyl Sepharose™ column.

The current results initially seem to show that the G50 size exclusion step is not effective, and it cannot be said to be as effective as affinity chromatography. Upon closer observation, an understanding of the purpose of the data reveals that it was relatively effective. The data purposely does not include most of the fractions with the highest specific activities, being fractions 11-13 and 15. This is because specific activity measurements were taken of fractions toward the sides of the curve seen in Figure 9, being fractions 8-10 and 16-21. To obtain a basic understanding of the extent of the purification fraction 14 had its full specific activity analyzed due to having the highest activity. The reason the size exclusion chromatography is less effective than affinity chromatography is because fraction 14 did not show a significantly increased specific activity.

Contrary to the project goals, the protein content did not seem to significantly decrease with the new purification process. In the size exclusion chromatography fractions, the fractions never reached the point of being below the threshold of detection for the Bradford assay, always being well within the range of the standard curve. This does not make sense. It would not account for the lack of reduction in total protein. More likely, the remaining contaminating proteins are of similar molecular weight.

The thermal stability experiment showed an encouraging level of stability of BSP of 60-70 °C, but the observed thermal stability of HRP was higher than expected. The literature showed a thermal stability of 40 °C in Figure 4 (Abdel-Aty et al., 2018), but the experimental stability was 50 °C. Regardless, it is obvious that BSP has a higher thermal stability than HRP. Nonetheless, the lower perceived thermal stability of HRP could have been the result of

differences in procedure. The only legitimate source of error in the experiment would be if the isotherms used did not actually bring the sample to the desired temperature, leading to a perceived higher thermal stability. The thermometers were not calibrated and, if they had error in their measurements, the perceived temperature would also be affected. Even with this, the comparative part of the experiment showed significantly higher thermal stability of BSP than HRP, which is a property that could be utilized in industrial applications like biosensors or analytical and diagnostic kits.

Future Research

Butternut squash peroxidase continues to appear promising as a candidate for industrial use. Nonetheless, more refinement of the purification scheme needs to be done to present a sample ready to have its properties characterized. Most of the general enrichment process has been carried out, leading to an increasingly purified sample. Another purification procedure that could be carried out is ion exchange chromatography. This process is also known as salting out chromatography, in which nonorganic electrolytes are run through such ion-exchange resins with salt solutions as eluents (Rieman, 1961).

Once the general enrichment process has been done the only compounds left should be proteins, and gel filtration can be used to separate many of them through the use of a gel specific to the size of butternut peroxidase. If in the end there are only one or two contaminants (proteins) left, then they can be characterized and targeted for removal.

Once purified, there is an endless fountain of information to be gleaned about BSP including its characterization, applications, and process of industrial purification and preparation. Even outside of BSP significant research is still yet to be done as to more specialized peroxidases (Twala et al., 2020).

Conclusion

The purpose of this research was to develop a purification scheme and analysis of the potential value of butternut squash peroxidase. With the main enrichment steps of the purification scheme complete and experimental proof of the increased thermal stability of BSP, both goals have been achieved. Due to the prevalency of butternut squash growing infrastructure due to its use as a food source, having a use for the skin which is usually just disposed of would yield extra profit. Upon further purification development and characterization, the possibilities for the use of peroxidase generally and BSP specifically truly seem to surpass that of many enzymes currently used.

References

Abdel-Aty, A. M., Hamed, M. B., Gad, A. A. M., El-Hakim, A. E., & Mohamed, S. A. (2018). Ficus sycomorus latex: An efficient alternative egyptian source for horseradish peroxidase in labeling with antibodies for immunodiagnostic kits. *Veterinary World*, *11*(10), 1364–1370. https://doi.org/10.14202/vetworld.2018.1364-1370

Alegria-Schaffer, A., Lodge, A., & Vattem, K. (2009). Performing and optimizing western blots with an emphasis on chemiluminescent detection. *Methods in Enzymology*, *463*, 573–599. https://doi.org/10.1016/S0076-6879(09)63033-0

Barber-Zucker, S., Mindel, V., Garcia-Ruiz, E., Weinstein, J. J., Alcalde, M., & Fleishman, S. J. (2022). Stable and functionally diverse versatile peroxidases designed directly from sequences. *Journal of the American Chemical Society*, *144*(8), 3564–3571. https://doi.org/10.1021/jacs.1c12433

Beyzavi, K., Hampton, S., Kwasowski, P., Fickling, S., Marks, V., & Clift, R. (1987). Comparison of horseradish peroxidase and alkaline phosphatase-labelled antibodies in enzyme immunoassays. *Annals of Clinical Biochemistry*, *24 (Pt 2)*, 145–152. https://doi.org/10.1177/000456328702400204

Bhalla, N., Jolly, P., Formisano, N., & Estrela, P. (2016). Introduction to biosensors. *Essays in Biochemistry*, *60*(1), 1–8. https://doi.org/10.1042/EBC20150001

Bischof, J. C., & He, X. (2006). Thermal stability of proteins. *Annals of the New York Academy of Sciences*, *1066*(1), 12–33. https://doi.org/10.1196/annals.1363.003

Biswas, P., Bharti, A., Kadam, A., & Dutt, D. (2020). Horseradish and potato peroxidase biobleaching of mixed office waste paper. *Bioresources*, *14*, 8600–8613. https://doi.org/10.15376/biores.14.4.8600-8613

Briley, K. (2021). The discovery and analysis of peroxidase enzyme in Pueraria montana. *Senior Honors Theses*. https://digitalcommons.liberty.edu/honors/1071

Gallati, H., & Pracht, I. (1985). [Horseradish peroxidase: Kinetic studies and optimization of peroxidase activity determination using the substrates H2O2 and 3,3',5,5'-tetramethylbenzidine]. *Journal of Clinical Chemistry and Clinical Biochemistry. Zeitschrift Fur Klinische Chemie Und Klinische Biochemie, 23*(8), 453–460.

Gore, S. (2017). The use of horse radish peroxidase, an eco-friendly method for removal of phenol from industrial effluent. *IOSR Journal of Environmental Science, Toxicology and Food Technology*, *11*, 07–13. https://doi.org/10.9790/2402-1103010713

Hiraga, S., Sasaki, K., Ito, H., Ohashi, Y., & Matsui, H. (2001). A Large Family of Class III Plant Peroxidases. *Plant and Cell Physiology*, *42*(5), 462–468. https://doi.org/10.1093/pcp/pce061

Jia, J., Wang, B., Wu, A., Cheng, G., Li, Z., & Dong, S. (2002). A method to construct a third-generation horseradish peroxidase biosensor: Self-assembling gold nanoparticles to three-dimensional sol-gel network. *Analytical Chemistry*, *74*(9), 2217–2223. https://doi.org/10.1021/ac011116w

Kokkinakis, D. M., & Brooks, J. L. (1979). Tomato peroxidase: Purification, characterization, and catalytic properties. *Plant Physiology*, *63*(1), 93–99. https://doi.org/10.1104/pp.63.1.93

Krainer, F. W., & Glieder, A. (2015). An updated view on horseradish peroxidases: Recombinant production and biotechnological applications. *Applied Microbiology and Biotechnology*, *99*(4), 1611–1625. https://doi.org/10.1007/s00253-014-6346-7

Leuenberger, P., Ganscha, S., Kahraman, A., Cappelletti, V., Boersema, P. J., von Mering, C., Claassen, M., & Picotti, P. (2017). Cell-wide analysis of protein thermal unfolding reveals determinants of thermostability. *Science (New York, N.Y.)*, *355*(6327), eaai7825. https://doi.org/10.1126/science.aai7825

Malik, V., & Pundir, C. S. (2002). Determination of total cholesterol in serum by cholesterol esterase and cholesterol oxidase immobilized and co-immobilized on to arylamine glass. *Biotechnology and Applied Biochemistry*, *35*(3), 191–197.

Mall, R., Naik, G., Mina, U., & Mishra, S. K. (2013). Purification and characterization of a thermostable soluble peroxidase from Citrus medica LEAF. *Preparative Biochemistry & Biotechnology*, *43*(2), 137–151. https://doi.org/10.1080/10826068.2012.711793

Min, K., Gong, G., Woo, H. M., Kim, Y., & Um, Y. (2015). A dye-decolorizing peroxidase from Bacillus subtilis exhibiting substrate-dependent optimum temperature for dyes and β-ether lignin dimer. *Scientific Reports*, *5*(1), 8245. https://doi.org/10.1038/srep08245

Nadaroglu, H., Celebi, N., Demir, N., & Demir, Y. (2013). *Purification and characterisation of a plant peroxidase from rocket (Eruca vesicaria sbsp. Sativa) (Mill.) (syn. E. sativa) and effects of some chemicals on peroxidase activity in vitro*.

Nuss, K., Perry, A., Anderson, E., Frommack, A., & Raner, G. (2021). Purification of peroxidase enzymes from various plant species. *Liberty University*.

Pandey, V., Awasthi, M., Singh, S., Tiwari, S., & Dwivedi, U. (2017). A comprehensive review on function and application of plant peroxidases. *Biochemistry & Analytical Biochemistry*, *6*. https://doi.org/10.4172/2161-1009.1000308

Pandey, V. P., & Dwivedi, U. N. (2011). Purification and characterization of peroxidase from Leucaena leucocephala, a tree legume. *Journal of Molecular Catalysis B: Enzymatic*, *68*(2), 168–173. https://doi.org/10.1016/j.molcatb.2010.10.006

Park, C. (2022). Visual interpretation of the meaning of kcat/KM in enzyme kinetics. *Journal of Chemical Education*, *99*(7), 2556–2562. https://doi.org/10.1021/acs.jchemed.1c01268

Passardi, F., Cosio, C., Penel, C., & Dunand, C. (2005). Peroxidases have more functions than a swiss army knife. *Plant Cell Reports*, *24*(5), 255–265. https://doi.org/10.1007/s00299-005-0972-6

Passardi, F., Penel, C., & Dunand, C. (2004). Performing the paradoxical: How plant peroxidases modify the cell wall. *Trends in Plant Science*, *9*(11), 534–540. https://doi.org/10.1016/j.tplants.2004.09.002

Ragland, B. D., Konrad, R. J., Chaffin, C., Robinson, C. A., & Hardy, R. W. (2000). Evaluation of a homogeneous direct LDL-cholesterol assay in diabetic patients: Effect of glycemic control. *Clinical Chemistry*, *46*(11), 1848–1851.

Rieman, W. I. (1961). Salting-out chromatography: A review. *Journal of Chemical Education*, *38*(7), 338. https://doi.org/10.1021/ed038p338

Sakharov, I. Y. (2001). Long-term chemiluminescent signal is produced in the course of luminol peroxidation catalyzed by peroxidase isolated from leaves of african oil palm tree. *Biochemistry. Biokhimiia*, *66*(5), 515–519. https://doi.org/10.1023/a:1010254801513

Savitski, M. M., Reinhard, F. B. M., Franken, H., Werner, T., Savitski, M. F., Eberhard, D., Martinez Molina, D., Jafari, R., Dovega, R. B., Klaeger, S., Kuster, B., Nordlund, P., Bantscheff, M., & Drewes, G. (2014). Tracking cancer drugs in living cells by thermal

profiling of the proteome. *Science (New York, N.Y.)*, *346*(6205), 1255784. https://doi.org/10.1126/science.1255784

Sharma, S. K., Sehgal, N., & Kumar, A. (2002). A quick and simple biostrip technique for detection of lactose. *Biotechnology Letters, 24*, 1737-1739. https://doi.org/10.1023/A:1020601400616

Šimonovičová, M., Tamás, L., Huttová, J., & Mistrík, I. (2004). Effect of aluminium on oxidative stress related enzymes activities in barley roots. *Biologia Plantarum*, *48*(2), 261–266. https://doi.org/10.1023/B:BIOP.0000033454.95515.8a

Singh, S., Pandey, V. P., Naaz, H., & Dwivedi, U. N. (2012). Phylogenetic analysis, molecular modeling, substrate–inhibitor specificity, and active site comparison of bacterial, fungal, and plant heme peroxidases. *Biotechnology and Applied Biochemistry*, *59*(4), 283–294. https://doi.org/10.1002/bab.1025

Spadiut, O., & Herwig, C. (2013). Production and purification of the multifunctional enzyme horseradish peroxidase. *Pharmaceutical Bioprocessing*, *1*(3), 283–295. https://doi.org/10.4155/pbp.13.23

Thongsook, T., & Barrett, D. M. (2005). Heat inactivation and reactivation of broccoli peroxidase. *Journal of Agricultural and Food Chemistry*, *53*(8), 3215–3222. https://doi.org/10.1021/jf0481610

Thorpe, G. H., & Kricka, L. J. (1986). Enhanced chemiluminescent reactions catalyzed by horseradish peroxidase. *Methods in Enzymology*, *133*, 331–353. https://doi.org/10.1016/0076-6879(86)33078-7

Twala, P. P., Mitema, A., Baburam, C., & Feto, N. A. (2020). Breakthroughs in the discovery and use of different peroxidase isoforms of microbial origin. *AIMS Microbiology*, *6*(3), 330–349. https://doi.org/10.3934/microbiol.2020020

Veljović Jovanović, S., Kukavica, B., Vidović, M., Morina, F., & Menckhoff, L. (2018). Class III peroxidases: functions, localization and redox regulation of isoenzymes. In D. K. Gupta, J. M. Palma, & F. J. Corpas (Eds.), *Antioxidants and Antioxidant Enzymes in Higher Plants* (pp. 269–300). Springer International Publishing. https://doi.org/10.1007/978-3-319-75088-0_13

Vreeke, M. S., Yong, K. Tsun., & Heller, Adam. (1995). A thermostable hydrogen peroxide sensor based on "wiring" of soybean peroxidase. *Analytical Chemistry*, *67*(23), 4247–4249. https://doi.org/10.1021/ac00119a007

Watanabe, Y., & Nakajima, H. (2016). Chapter twenty—creation of a thermally tolerant peroxidase. In V. L. Pecoraro (Ed.), *Methods in Enzymology* (Vol. 580, pp. 455–470). Academic Press. https://doi.org/10.1016/bs.mie.2016.05.038

Zhang, Y., Zhang, Y., Wang, H., Yan, B., Shen, G., & Yu, R. (2009). An enzyme immobilization platform for biosensor designs of direct electrochemistry using flower-like ZnO crystals and nano-sized gold particles. *Journal of Electroanalytical Chemistry*, *627*(1), 9–14. https://doi.org/10.1016/j.jelechem.2008.12.010

Zia, M. A., Kousar, M., Ahmed, I., Iqbal, H. M. N., & Abbas, R. Z. (2011). Comparative study of peroxidase purification from apple and orange seeds. *African Journal of Biotechnology*,*10*(33), 6300-6303. https://doi.org/10.5897/ajb10.2675